Biochemical Journal Immediate Publication. Published on 1 Nov 2002 as manuscript BJ20020935

Novel Mesenchymal and Hematopoietic Cell Isoforms of the SHP-2 Docking Receptor, PZR: Identification, Molecular Cloning and Effects on Cell Migration.

Andrew C.W. Zannettino[*†], Maria Roubelakis[‡§†], Katie J. Welldon[*], Denise E. Jackson[‖], Paul J. Simmons[¶], Linda J. Bendall[#], Anthony Henniker[#], Kate L. Harrison[*], Silvana Niutta[*], Kenneth F. Bradstock[#] and Suzanne M Watt[‡].

[*] Myeloma and Mesenchymal Research Group, Matthew Roberts Laboratory, Hanson Centre for Cancer Research, I.M.V.S., Adelaide 5000, Australia.
[‡]Stem Cell Laboratory, National Blood Service, and Nuffield Department of Clinical and Laboratory Sciences, University of Oxford, Oxford, OX3 9DU, United Kingdom.
[§]MRC Molecular Haematology Unit, Weatherall Institute of Molecular Medicine, University of Oxford, Oxford, OX3 9DS, United Kingdom.
[‖]Immunoreceptor Laboratory, Hanson Centre for Cancer Research, I.M.V.S., Adelaide 5000, Australia.
[¶] Human Stem Cell Laboratory, Peter MacCallum Cancer Institute, East Melbourne, 3002, Australia.
[#]The Millennium Institute, Westmead Hospital, University of Sydney, Westmead, 2145, Australia

[†] ACWZ and MR contributed equally to this manuscript and are joint first authors.

Correspondence and reprint requests to:
Suzanne M. Watt Ph.D.,
Stem Cell Laboratory,
National Blood Service,
Oxford Centre, The John Radcliffe Hospital,
Headington, Oxford, OX3 9DU, UK.

Phone: +44 (0) 1865 447919
Facsimile: +44 (0) 208 9985174
E-mail: Suzanne.watt@nbs.nhs.uk

Running Title: Novel PZR Isoforms in the Hematopoietic System.

Abbreviations: SHP-1; src homology phosphatase type 1, SHP-2; src homology phosphatase type 2, PZR; protein zero related, c-Kit; steel factor receptor, CAMs, cell adhesion molecules; HPC, hematopoietic progenitor cells; BFU-E, blast forming unit-erythroid; CFU-GM, colony forming unit-granulocyte/macrophage; HBMSC, human bone marrow stromal cells; BM, bone marrow; IgSF, Immunoglobulin superfamily. IGF-1, insulin growth factor-1; SHPS-1, SHP-substrate 1; HUVEC, human umbilical vein endothelial cells; mAb, monoclonal antibody; PE, phycoerythrin; FITC, fluorescein isothiocyanate; NGS, normal goat serum, Ig immunoglobulin; ITIM, immunoreceptor tyrosine-based inhibitory motif.

Biochemical Journal Immediate Publication. Published on 1 Nov 2002 as manuscript BJ20020935

SYNOPSIS

SHP-2 is essential for hematopoietic skeletal and vascular development. Thus, the identification of its binding partners is critically important. Here, we describe a unique monoclonal antibody, WM78, which interacts with PZR, a SHP-2 binding partner. Furthermore, we identify two novel isoforms of PZR, PZRa and PZRb, derived by differential splicing from a single gene transcription unit on human chromosome 1q24. All are type 1 transmembrane glycoproteins with identical extracellular and transmembrane domains, but differ in their cytoplasmic tails. The PZR intracellular domain contains two SHP-2 binding ITIM-motifs ($VIY^{246}AQL$ and $VVY^{263}ADI$) which are not present in PZRa and PZRb. Using the WM78 monoclonal antibody (mAb) to the common extracellular domain of the PZR isoforms, we demonstrate that the PZR molecules are expressed on mesenchymal and hematopoietic cells, being present on the majority of $CD34^+CD38^+$ and early clonogenic progenitors and at lower levels on $CD34^+CD38^-$ cells and the hierarchically more primitive pre-CFU. Interestingly, we show, by RT-PCR, that the PZR isoforms are differentially expressed in hematopoietic, endothelial and mesenchymal cells. Both PZR and PZRb are present in $CD133^+$ precursors and endothelial cells, PZRb predominates in mesenchymal and committed myelomonocytic progenitor cells and all three isoforms occur in erythroid precursor cell lines. Importantly, using SHP-2 mutant (Δ46-110) and SHP-2 rescue embryonic fibroblasts stably expressing the PZR isoforms, we demonstrate for the first time that PZR, but not PZRa or PZRb, facilitates fibronectin dependent migration of cells expressing a competent SHP-2 molecule. These observations will be instrumental in determining the mechanisms whereby PZR isoforms regulate cell motility.

Key words: Immunoglobulin superfamily; $CD34^+$; stem cells; function; genomic structure.

Biochemical Journal Immediate Publication. Published on 1 Nov 2002 as manuscript BJ20020935

INTRODUCTION

Complex processes such as cell growth, differentiation, and migration require the integration of multiple types of extracellular signals, including those delivered by growth factors, cytokines, cell adhesion molecules and extracellular matrix (ECM) proteins [1]. Most signaling pathways involve changes in cellular tyrosyl phosphorylation which are regulated by a diverse family of protein tyrosine kinases (PTKs) and an equally diverse family of protein tyrosine phosphatases (PTPs) [2]. SHP-1 and SHP-2 comprise a subfamily of tyrosine-specific cytoplasmic PTPs, with roles in hematopoiesis, bone formation and vasculogenesis [3-6] . Whilst SHP-1 and SHP-2 share approximately 60% overall sequence identity, contain two SH2 domains and a catalytic domain, they exhibit distinct physiological functions. SHP-1 is predominantly expressed in haematopoietic cells and is a negative regulator of phosphotyrosine signaling [7-9], whereas SHP-2 is ubiquitously expressed and is considered to be a positive mediator of hematopoiesis [4, 8, 10, 11]. These molecules are cytoplasmic tyrosine phosphatases, each containing two unique SH2 domains which bind to a distinct amino acid sequence surrounding a phosphotyrosine residue.

Evidence for the functional importance of SHP-1 and SHP-2 comes from the analyses of *shp-1* and *shp-2* mutant knock-out organisms. SHP-1 *motheaten* (me) and *motheaten viable* (me^{v}) [7] mice suffer from immune deficiency and autoimmune diseases and exhibit hematopoietic abnormalities, e.g. excessive erythropoiesis, augmented granulocyte and monocyte production and tissue accumulation, overexpansion of $CD5^{+}$ B cells, leukocyte hypersensitivity and deregulated mast cell and defective T and NK cell functions [7, 10, 12]. In contrast, disruption of the mouse SHP-2 gene causes death of the embryos at midgestation, highlighting its importance in development. Moreover, fibroblasts from mice harbouring a deletion of SHP-2 exon 3, which express low levels of a defective SHP-2 protein that lacks its N-terminal SH2 domain [13] exhibit impaired mitogen-activated protein kinase (MAPK) activation in response to fibroblast growth factor (FGF), epidermal growth factor (EGF), and insulin-like growth factor I (IGF-I) [13, 14]. In other pathways, however, SHP-2 binds to distinct signaling intermediates. One class of SHP-2 binding proteins, exemplified by the *Drosophila daughter of sevenless* (*dos*) gene product, consists of an N-terminal pleckstrin homology domain, multiple proline-rich stretches and potential tyrosyl phosphorylation sites [15]. A second class of molecules belonging to the Ig-ITIM (Immunoglobulin-Immunoreceptor Inhibitory Motif) family has been identified as SHP-2 binding proteins. SHP substrate 1 (SHPS-1) is a prototypical member of this class of receptors, of which there are now more than 30 proteins. This family is characterised by the presence of one or more ITIMs (comprising of 6 amino acids (I/V/L/S)xYxx(L/V)) in their cytoplasmic domain. The consensus motif is nearly always associated with a second tandem ITIM, separated from the first by a canonical 25-31 amino acid long spacer sequence [16]. SHPS-1 was initially identified as a SHP-

2 binding protein, the tyrosyl phosphorylation of which is increased in cells expressing catalytically impaired SHP-2 mutants.

In an attempt to identify additional substrates for SHP-2, Zhao and Zhao [17] overexpressed a catalytically inactive mutant of SHP-2 in HEK-293 cells. Following pervanadate stimulation, several hyper-tyrosine phosphorylated glycoproteins associated with SHP-2 were identified, including a 43-kD membrane protein [17].The protein was subsequently purified to homogeneity and amino acid sequence derived. Based on this sequence, a full length cDNA was isolated and found to encode a novel transmembrane protein, which they termed PZR (Protein Zero Related) due to its significant homology to the major structural protein of peripheral myelin, myelin P0. The extracellular domain of this protein contains a single extracellular Ig domain and two intracellular ITIMs ($VIY^{241}AQL$ and $VVY^{263}ADI$). Using site-directed mutagenesis, these workers demonstrated that these two ITIMs accounted for the entire tyrosine phosphorylation of PZR and were essential for SHP-2 recruitment and activation [18]. Like SHPS-1, PZR was found to be widely expressed. However, it specifically interacts with SHP-2 but not with SHP-1 [18].

In this paper, we describe a unique mAb, WM78, that reacts with the extracellular domain of human PZR. Expression cloning using this mAb and RT-PCR analysis have identified two novel PZR isoforms, PZRa and PZRb, both lacking ITIM motifs. We further demonstrate the differential expression of these isoforms in cells of hematopoietic and mesenchymal origin. Genomic analysis and *in silico* cloning demonstrate that these three isoforms are transcribed from a single gene transcription unit on human chromosome 1q24. Interestingly, these novel isoforms differentially regulate fibronectin-mediated cell motility in a SHP-2 dependent manner.

EXPERIMENTAL

Cells and WM78 Monoclonal Antibody Generation

Human hematopoietic cell lines, have been described earlier. HUVEC cells were provided by Drs. I. Rappold and M. Raida. Peripheral blood (PB), posterior iliac crest bone marrow (BM) and umbilical cord blood (UCB) mononuclear cells were collected with informed consent and ethical approval [19-21]. U937 cells were cultured in 10% FCS RPMI-1640 medium containing 10^{-7} M 12-O-tetradecanoylphorbol 13-acetate (TPA) (Sigma Chemical Co) as a differentiating agent for 4 days to induce monocytic differentiation characterised using α-naphthyl acetate non specific esterase staining [22]. The WM78 mAb was derived after immunization of BALB/c mice with the human T cell line, 8402, and fusion of spleen cells with the SP2/0 myeloma cell line [23].

Human Bone Marrow Stromal Cell (HBMSC) and Human Bone Marrow Stromal/Osteoblast (SOB) Cell Cultures and Magnetic Bead Isolation.

Stromal cultures were established from BMMNC [24]. Trabecular bone specimens were obtained from the Department of Orthopaedic and Trauma, Adelaide Hospital with informed consent and institutional ethical approval. Single cells were prepared by collagenase (3mg/ml; collagenase Type I; Worthington Biochemical Co., Freehold, NJ) and dispase (4mg/ml; neutral protease grade II; Boehringer-Mannheim) treatment. Cell suspensions were analyzed by CD14 and CD45 staining (FACS or immunofluorescence) and showed no contamination with macrophages or hematopoietic cells [19-21]. BMMNC were incubated with CD34 (561) Dynabeads (Dynal, Oslo, Finland) and $CD34^+$ cells captured magnetically and recovered with DETACHaBEAD^{TM} reagent (Dynal). $CD34^+$ and $CD133^+$ UCB and PB monocytes were also isolated with $CD34^+$, $CD133^+$ or $CD14^+$ magnetic beads, respectively (Miltenyi-Biotech, Bergish, Gladbag. Germany) [20, 21]. Isolated were labeled with CD34-PE (phycoerythrin), AC133/2-PE or CD14-PE mAbs and were routinely >95% pure.

In Situ Immunofluorescence Staining

HBMSC cultured in 8-chamber slide flasks (Nunc Inc. Naperville, IL), were fixed in acetone/methanol (1:1), blocked with 5% (v/v) normal goat serum (NGS) and stained with the WM78 mAb or an isotype-matched mIgG1 control followed by FITC (fluorescein isothiocyanate) - conjugated goat anti-mouse $F(ab)_2$ Ig (Silenius, Hawthorn, Vic., Australia) [20]. Cells were examined under an Olympus BH2-RFCA fluorescence microscope (Olympus Microsystems, London, England).

Flow Cytometry and sorting

For single color analyses, cells were stained as described [21]. For dual color analyses, cells were labeled with CD4-PE, CD8-PE, CD56-PE or CD19-PE plus biotinylated WM78 mAb and streptavidin-FITC or with CD14-FITC, CD45-FITC, CD19-FITC, CD15-FITC or glycophorin A-

FITC, followed by WM78-biotin plus streptavidin-PE or CD3-PE followed by WM78-biotin plus streptavidin-FITC [21]. For triple color labeling, cells were stained with CD34-FITC (clone 8G12) and CD38-PE (clone HB-7), plus WM78-biotin and streptavidin-tricolor (TC; Caltag Laboratories, Burlingame, CA) [20]. BMMNCs were FcR blocked and stained with CD34-PE (clone 8G12) and WM78-biotin followed by streptavidin-TC and sorted on the FACStar^{PLUS} (Becton-Dickinson, Sunnyvale, CA) [23].

Clonogenic Assays and Pre-Progenitor Cell (Pre-CFU) Culture

Cells were assayed for day 14 granulocyte-macrophage (CFU-GM), and/or granulocyte (CFU-G) and macrophage (CFU-M) colony forming cells, early erythroid progenitors (BFU-E) and multipotential colony forming cell (CFU-Mix) in semi-solid methylcellulose cultures [19, 23]. All colonies were scored according to standard criteria after 14 days incubation. Sorted cells were cultured in pre-CFU medium containing a cocktail of six haematopoietic growth factors (6HGF) rhu IL-1, IL-3, IL-6, G-CSF, GM-CSF and SCF, all at 10 ng/ml, for 28 days [25].

Immunoprecipitation and SDS –PAGE

Goat anti-mouse Ig-coupled Dynabeads (Dynal) were pre-armed with purified immunoglobulin (WM78 and isotype matched non-binding controls) as described previously [26]. Samples were run on 10% (w/v) SDS-polyacrylamide gel electrophoresis (SDS-PAGE) [27], transferred to polyvinyl-difluoroacetate membranes (PVDF; MSI Membranes, Bresatec, Adelaide, Australia) and developed with streptavidin-alkaline phosphatase (AP; Amersham Int, Little Chalfton, Berks., England). Immunoreactive proteins were resolved using a FluorImager and ImageQuant software (both from Molecular Dynamics, Sunnyvale, CA).

Expression Cloning and Sequencing of the WM78 cDNA Clone

The PZRa cDNA was isolated from a human bone marrow stromal cell (HBMSC) cDNA library in the retroviral vector pRUFneo [23] using the WM78 mAb. Following PCR recovery of proviral cDNA inserts from genomic DNA, unique Bam HI and Xho I restriction sites present in the 5' and 3' flanking regions respectively were used to reclone the cDNA into pRUFneo. Stable G418 resistant $\Psi 2$ virus-producing cell lines were produced by calcium phosphate transfection and used to infect FDCP-1 cells by co-cultivation [28]. G418 resistant FDCP-1 cells were analyzed for antigen expression by indirect immunofluorescence, flow cytometry and immunoprecipitation as above.

Identification of Full Length PZR, PZRa and PZRb cDNAs and Real Time Quantitative PCR

Marathon-ready human Burkitt's lymphoma (Raji cell line) cDNA was purchased from Clontech Laboratories Inc., Palo Alto, CA. Total RNAs from cell lines described above, and from normal stromal/osteoblast cells, CD133$^+$, CD34$^+$, CD14$^+$ and HUVEC cells, extracted using the RNAzol (Biogenesis, Ltd, Poole, England) and the RNA easy (Qiagen Ltd, West Sussex, England) reagents,

were reverse transcribed using Sensiscript Reverse Transcriptase system (Qiagen Ltd.). Human PZR, PZRa and PZRb were generated by PCR amplification of the cDNAs described above using appropriate forward and reverse primers (Sigma Chemical Co.) and the Expand^{TM} Long PCR system (Boehringer-Mannheim) [19]. The cDNAs were ligated into the pGEM-T easy vector (Promega) and PCR amplified using the Expand^{TM} Long Template System (Boehringer-Mannheim) and PUC M13 forward and reverse primers [19]. The PZR, PZRa and PZRb PCR products were sequenced automatically on an ABI 377 Automatic Sequencer (Perkin-Elmer-Applied Biosystems) [19]. Peptide motifs and structural characteristics were predicted using TopPred 2, Das, Signal P, TMHMM, O-Glycbase, Net Phos 2.0 Server and MacVector software packages [19].The PZR and PZRb TaqMan^{TM} (Applied Biosystems) systems consist of the the following pair of primers: FPZR (635) T T A A G C A G G C T C C T C G G A G T, RPZR(742) C G G A G T G G T C T A A C T G T G C A T A T A T G and FPZRb (574) A G A A G G A A A A A C T C T A A A C G G A T T, RPZRb (688) G C A T A C A C C A C A G A C T C T G A C T T G T' respectively as well as dual fluorescent probes (PZR: 5'C C C T C C G A C A C T G A G G G T C T T G T A A A G A G T C'3 and PZRb: 5'A A C T G T G C A T A T A T G A C T G G G C C C C A G T '3). PZRa was not quantified by this method because it was not found in high levels in the majority of cells tested and because the sets of primers and fluorescent probes that can be designed in the region that distinguish PZRa from the other two isoforms (the 3' part of exon 4) can amplify genomic DNA. The reaction was set up as described in Chiu et al [29]. The difference in the levels of expression between PZR and PZRb in different haematopoietic cells was given by the ΔCt value: ΔCt=| CtPZR - CtPZRb|. The relative expression ratio between the two molecules was calculated using the following formula: $2^{|\Delta Ct|}$. All the experiments were carried out in duplicate on 4 independent occasions.

PZR Genomic PAC and Cosmid DNA Clones and Southern Blots

Three PZRa cDNA probes were used for screening human genomic libraries and subclones and for Southern blotting (see Figure 7). Probe A used for screening a human leukocyte PAC library was derived from the BamHI/XhoI fragment of PZRa cDNA in the pGEM-T vector. Probe B (366bp), used to probe the human chromosome 1 specific cosmid library, was generated by BamHI and Hind II digestion of the PZRa cDNA, while probe C was a PCR product generated from the PZRa. Each cDNA probe was labeled with 30μCi α-^{32}P-dCTP (Amersham Int.) using the T7 Quickprime kit (Pharmacia-Biotech AB) or with the DIG labeling kit (Roche Diagnostics, Mannheim, Germany) [19, 20]. The human PAC library was hybridized with α-^{32}P-labeled probe A. Nine positive PAC clones identified from these filters or by using the Human Genome Blast program (NCBI Genome Sequencing Centre) for PAC clones. 313-L4 PAC clone was selected for further analysis. A human chromosome 1 specific cosmid library LLNL Human (HGMP Resource Centre) was probed with PZRa probe B. Seven cosmid DNA clones were isolated and then analysed using the PZRa probe B

or PCR amplified using a range of primer pairs and the ah95b1 cosmid clone was selected for detailed analysis. Human PAC, cosmid and human leukocyte genomic DNA (Promega) samples were further analysed using PZRa probes A, B or C (see Figure 7) labeled with α-^{32}P-dCTP or with DIG (Roche Diagnostics) [19]. PAC and cosmid DNAs were analyzed by PCR amplification using appropriate primers, the Expand^{TM} Long PCR System (Boehringer Mannheim) and the PCR program described above. Human genomic DNA was PCR amplified as above in order to verify the PZR genomic sequence in the PAC and cosmid clones. PCR amplification for the GC 5' rich region of the gene used the Advantage-GC Genomic Polymerase mix (Clontech Ltd., Cambridge, Cambridgeshire, England) with 95^{0}C for 1 min. 25 cycles of 94^{0}C for 30 secs. and 68^{0}C for 12 mins. and 1 cycle of 68^{0}C for 12 mins. The PCR products were isolated by agarose gel electrophoresis and ligated into the pGEM-T vector for sequencing.

Fluorescence in situ Hybridization (FISH) and In silico cloning

Metaphase spreads were prepared from phytohemagglutinin-stimulated normal human lymphocytes probed with the biotinylated ah95b1 cosmid clone as described previously[21]. Neither exon 1 nor and the first 1.5 kb of intron 1 were present in the 313-L4 PAC or ah95-b1 cosmid clone sequences. Since we located the PZR gene on human chromosome 1q24, and since the Homo Sapiens chromosome 1 working draft sequence had been determined by the Sanger Centre and provided by the NCBI, the sequence of exon 1 and intron 1 was identified in silico (Genbank database, Accession number: NT004668).

Production of MEF cell lines stably expressing PZR isoforms

Mouse embryonic fibroblasts (MEFs) were used as SHP-2$^{-/-}$ MEF cells lacking the intact N-SH2 domain (Δ46-110) or as "wild type" (SHP-2 rescue) MEF cells in which the (Δ46-110) mutant MEF cell line was stably transfected with a competent SHP-2 gene. PZR, PZRa and PZRb were RT- PCR amplified from KG1A and HUVEC cells. The cDNAs were digested with BamHI and XhoI and subcloned into the multiple cloning site of the pRUF. Neo retroviral vector and transfected into the ψ_2 [23]. Cells were selected in 400µg/ml G418 prior to transfer into G418 free medium DMEM for virus collection and retroviral infection of the MEF cells [23]. Flow cytometry and immunoprecipitation identified PZR, PZRb and PZRa proteins of 48, 36 and 34 kD using the WM78 mAb (data not shown). The top 50% of the cells expressing PZR were isolated by flow sorting as above, cultured in 400µg/ml G418 and used in the migration assay[23].

Migration Assay

The underside of transwell 8µm pore filter was coated in triplicate with either 1 ml of 10µg /ml fibronectin (Boehringer Mannheim) or 10µg/ml BSA as a control, for 2 hours at 37^{0}C or overnight at 4^{0}C. Twenty four hours prior to seeding the cells onto the transwell filter (Costar® Corning, NY, USA) the cell lines were split 1:2 to ensure log phase growth and 5x10^4 cells in serum free DMEM

added to the upper chamber of the transwells. 500µl of serum free media containing 4µg/ml of fibronectin was added to the lower chamber and incubated at 37^0C for 5 hours. Cells which migrated through the filter were fixed in 3.7% (w/v) paraformaldehyde for 10 mins and stained with 0.2% (w/v) crystal violet in ethanol (ICN Biomedicals, Inc., Costa Mesa, CA, USA) for 20 mins at room temperature Crystal violet was extracted using 300µl of 10% (v/v) acetic acid for 5 mins at room temperature on a shaker. The results were quantified using a Beckman D4-65 spectophotometer at 600nm wavelength. Data points derived from 3 independent experiments are reported as the mean ± standard error of the mean (SEM). Analysis of the variance to determine significant differences between treatments was performed using ANOVA Factorial analyses.

RESULTS

The Monoclonal Antibody WM78 Identifies an Antigen Expressed by Bone Marrow Mesenchymal and Peripheral Blood Mononuclear Cells

The WM78 mAb was selected for its reactivity with bone marrow derived mesenchymal or cultured stromal/osteoblast cells (Figure 1a). However, its reactivity was not restricted to these cells. Figure 1b illustrates that WM78 binds more strongly to peripheral blood monocytes than to granulocytes, platelets and erythrocytes. Indeed, in 3 independent experiments, median fluorescence intensities (MFI) of 395.3±55.5 (mean ±S.E.M.) for $CD14^+$ monocytes, 19.8±5.4 for $CD15^+$ granulocytes, 16.4±5.4 for $CD41b^+$ platelets and 12.7±4.2 for glycophorin A^+ erythrocytes were obtained, compared with negative isotype control MFIs of 2.9±0.5, 2.9±0.5, 2.5±0.5 and 3.4±0.5, respectively. Within the lymphoid compartment, the expression of the WM78 defined antigen was variable, ranging from negative or low to strongly positive. Figure 1c illustrates the percentage of $CD14^+$ monocytes, $CD19^+$ B cells, $CD4^+$ and $CD8^+$ T cells, and $CD56^+$ NK cells staining with WM78. In adult human bone marrow, a similar phenomenon was observed as illustrated in Figure 2.

WM78 Differentially Binds to $CD34^+$ Cell Subsets and Hematopoietic Precursors

A uniform level of WM78 mAb binding was found on most $CD34^+$ bone marrow precursor cells, with 91.9±3.2% (mean ±S.E.M., n=3) of these cells occurring in the $CD34^+WM78^+$ gate (Figure 3a A). Within this $CD34^+$ population, the $CD34^+CD38^+$ cells expressed higher levels of the WM78 defined antigen than did the more primitive $CD34^+CD38^{lo/-}$ subset as determined by three color flow cytometric staining (Figure 3a B and C). For example, WM78 MFIs of 54.7±3.5, 22.4±1.5 and 2.3±0.5 (means±S.E.M., n=3) were obtained for the $CD34^+CD38^+$, $CD34^+CD38^{lo/-}$ and isotype matched negative control subsets, respectively. To confirm that the WM78 mAb bound to committed hematopoietic progenitor cells, *in vitro* clonogenic and pre-CFU assays were performed on BMMNC-derived FACS isolated $CD34^+$ (Region R1), $CD34^+WM78^+$ (Region R2) and $CD34^+WM78^-$ (Region R3) cells (Figure 3b A). The majority of day 14 BFU-E and CFU-E, were recovered in the $WM78^+CD34^+$ fraction (Region R2 of Figure 3b A). FACS isolated (Figure 3b A) $CD34^+WM78^+$ (Region R3) and $CD34^+WM78^-$ (Region R2) or $CD34^+$ (Region R1) fractions were also assayed for *de novo* generation of nucleated cells in the pre-CFU assay (Figure 3b C). When 1000 cells were cultured, all the three $CD34^+WM78^+$ and $CD34^+WM78^-$ or $CD34^+$ cell subsets were able to generate nucleated cells.

WM78 Identifies PZRa, a Novel ITIM-less Isoform of the SHP-2 Binding Partner PZR

Given its reactivity with a cell surface molecule on cultured human BM stromal cells (Figure 1a), the WM78 mAb was used to screen a human bone marrow stromal cell cDNA expression library in the retroviral vector pRUF.*neo*. Automatic sequencing of the resultant cDNA and Genbank/EMBL

database analyses revealed substantial nucleotide homology to the previously cloned PZR molecule that is expressed in epithelial cells [17]. We named this molecule PZRa (Genbank accession number AF181660). Expression of PZRa cDNA in the murine hematopoietic progenitor cell line FDCP-1, (Figure 4a B) and immunoprecipitation using the WM78 mAb identified a protein with an apparent molecular mass of approximately 30kD (Figure 4b, lane B). Comparative nucleotide and predicted amino acid sequences of PZRa with PZR are shown in Figure 5 and demonstrate type 1 transmembrane molecules with identical extracellular and transmembrane domains but different cytoplasmic tails.

Identification of PZR Isoforms in Hematopoietic, Endothelial and Mesenchymal Cells

Since our studies revealed that PZR and PZRa contained different cytoplasmic sequences but identical extracellular and transmembrane domain sequences, we PCR amplified cDNAs using an identical forward primer (FPZR positioned at -17 from the ATG) but different reverse primers to sequences in the 3' UTRs that would specifically distinguish between PZR and PZRa gene products, namely R904 and R974 repsectively (Figure 5). Initial PCR analyses, using these primer pairs with the Raji and KG1A cDNAs, generated three rather than two different products. One product of approximately 650 bp produced with the primer pair, FPZR and R904, was detected only after 60 cycles of PCR amplification and was identical to the PZRa sequence (Figure 5). The other two products that were generated using the primer pair FPZR and R974 were approximately 900 and 700 bp in size and were generated with 30 cycles of PCR amplification (Figure 6a). Sequence analysis demonstrated that the larger product was identical to PZR (Figure 5) whereas the smaller product was identical to PZR in its extracellular and transmembrane domains, but not in its cytoplasmic tail. We have termed this product, PZRb (Figure 5). Further RT-PCR analysis revealed that the PZR and PZRb isoforms are widely expressed in the hematopoietic progenitor cells and cell lines examined (Figure 6a). Using real-time quantitative PCR, it was found that PZR and PZRb were present in almost equivalent amounts in $CD14^+$ peripheral blood monocytes and in cell lines representing pre B (RPMI-1788). However, PZRb appeared to be the major isoform in $CD34^-$ promyelocytic (HL60) and promonocytic (U937) cell lines (7.31 and 7.11 fold higher expression, respectively than PZR) and in multipotent progenitor cells (KG1A). Differentiation of U937 cells along the monocytic lineage revealed a decrease in PZRb and an increase in PZR expression. Interestingly, PZR was prominent in stromal cells (23.1 fold higher than PZRb) and to a lesser extent in human umbilical vein endothelial cells (HUVEC) and in erythroid progenitors (K562) (Figure 6b). The PZRa isoform was expressed at significant levels (i.e. using 30 cycles of RT-PCR amplification) in the erythroid progenitor cell line K562, but was detected only after 60 PCR cycles and therefore at putatively low levels in KG1A and Raji cells (Figure 6a and data not shown). The differential distribution of the PZR isoforms in different cell types suggests that a mechanism exists for controlling PZR isoform expression and hence function during lineage development or commitment within the hematopoietic, mesenchymal and vascular systems. Since FACS analysis

(see Figures 1 to 3) revealed that WM78 binds strongly to mesenchymal derived cells and to a variety of hematopoietic cells and their progenitors, we immunoprecipitated the WM78 defined molecule from human bone marrow stromal/osteoblast (SOB) cells (Figure 6c, lane D), bone marrow $CD34^+$ cells (Figure 6c, lane E) and the erythroid progenitor cell line K562 (Figure 6c, lane F). The results demonstrated the presence of multiple protein bands on SDS-PAGE gels under reducing conditions. A major band with an apparent molecular mass of approximately 32-36 kD was found in the SOB cell lysate and was weakly detectable in K562 cells, which like bone marrow $CD34^+$ progenitor cell lysates, produced a main band at approximately 36-48kD. The latter is identical to the molecular mass previously identified for PZR in transfected cells [17], while the former 32-36kD band in SOB cells is likely to represent PZRb. These studies suggest that the different PZR isoforms are differentially expressed in hematopoietic and mesenchymal derived cells.

Amino acid Sequence Identity and Potentially Important Motifs for the PZR Isoforms

The amino acid sequence similarities and predicted structures of the three PZR-like peptides are shown in Figures 5, 6d and e respectively. PZRa, PZRb and PZR cDNAs are predicted to encode type 1 transmembrane proteins of 202, 209 and 269 amino acids, respectively. In all three isoforms, the predicted signal peptide cleavage site is positioned between Arg 37 and Leu 38 (VSA-LE). An IgV-set domain motif linked by disulfide bridges is predicted to occur between amino acids 58 and 135, placing these molecules in the immunoglobulin (Ig) superfamily. Each PZR isoform contains two potential N-linked glycosylation sites (at Asp 50 and Asp 130) and three potential O-linked glycosylation sites at Thr 70 and on Ser residues 70 and 75. A 27 amino acid transmembrane hydrophobic sequence lies between amino acids 162 and 189. PZR possesses the longest intracellular domain of 80 amino acids, and contains a classical ITIM motif of the type (V/I)*XYXX*(L/V) and more specifically $VIY^{246}AQL$ and $VVY^{263}ADI$ (246 and 263 tyrosine phosphorylation sites) that has previously been shown to interact with the SH2 domains of SHP-2 [17, 18]. The cytoplasmic domains of PZRa and PZRb are truncated to 13 and 20 amino acids respectively with both lacking the classical ITIM motif and SHP-2 binding sites. Database analyses revealed one potential tyrosine phosphorylation site at position 200 of the amino acid sequences in both PZRa and PZRb molecules. PZR isoforms show significant amino acid similarity with myelin Po protein and epithelial V-like antigen 1 (Figure 6e).

Genomic Structural Analyses Reveal that the PZR Isoforms are Derived by Differential Splicing of a Single Gene Transcription Unit and are Located on Human Chromosome 1q24

To determine if the PZR isoforms are products of one or more genes, we analyzed the genomic structure. The 313-L4 PAC clone (Genbank Accession number: Z99943) provided a partial sequence for the PZR gene that we predict encompasses part of intron 1 and exons 2 to 6 but lacks the 5' region encompassing the signal sequence and 5' that would exon 1. The exon 1 and intron 1

sequences (GenBank Accession number: NT004668) were identified using an *in silico* cloning strategy. Comparative analyses of the genomic sequence with PZR, PZRa and PZRb cDNAs indicated that these isoforms are derived by differential splicing of exons from a single gene transcription unit (Figure 7b). The region spanning the coding exons 1 to 6 covers at least 66 kb of genomic DNA. While the PZR isoforms are identical from exon 1 to 4, the sequences of the isoforms diverge in subsequent exons. The signal peptide is encoded by exon 1 and part of exon 2, while the extracellular region is encoded by exons 2 and 3 and part of exon 4 (111- 482 nt). The transmembrane sequence is encoded by exon 4 (483-567 nt). For the PZRa transcript, exon 4 begins at +473 bp from the ATG of the translational start site with a TAA stop codon at bps +607 to +609. This is followed by a 3' UTR sequence of at least 541bp. Similarly, for both the PZR and PZRb transcripts, exon 4 starts at +473 bp and reads through to +605 bp. However, unlike PZRa, both PZR and PZRb then use a dinucleotide GT splice site one base before the stop codon of PZRa to splice onto additional exons. PZR splices onto exon 5, which comprises 103 bps and covers +606 to +705 bps of the mRNA sequence, which then splices onto exon 6 which encompasses +706 to +1019 bps, with a TAA stop codon located at +808 to +810 bps. PZRb splices from exon 4 onto exon 6 at +606 bp but reads through to a TAG stop codon at +628 bp. From the cDNA sequence, we would predict a minimum 3' UTR sequence of 123 bp. Metaphase spreads were examined using the 95b1 cosmid clone containing the PZR gene as a probe. Positive signals were observed on both chromatides of human chromosome 1 at band 1q24 (Figure 8).

PZR, but not PZRa or PZRb, Regulates Integrin-Mediated Cell Motility

Stable transfectants were analysed for their relative expression levels of the PZR isoforms using flow cytometry with the WM78 mAb. A representative set of histograms (Figure 9a) shows a relatively uniform mean fluoresence intensity for each of the transfectants. Using these cells, we investigated the effects of SHP-2 depletion in relation to PZR and its various isoforms on migration over the extracellular matrix protein, fibronectin. Previous studies have indicated that the SHP-2 mutant cells (Δ46-110) migrate at a slower rate than the SHP-2 rescue cells [30] and that the mutant SHP-2 protein without the intact N-SH2 domain (Δ46-110) does not function in a dominant negative manner but rather as a loss-of-function molecule [14]. Thus, the availability of the SHP-2 rescue, “wild type” fibroblast cell line, where SHP-2 had been re-introduced into SHP-$2^{-/-}$ cells together with the homozygous SHP-$2^{-/-}$ mutant (Δ46-110) fibroblast cell line, provided us with a unique opportunity to study PZR-mediated effects in a SHP-2 positive or negative background. Using a transwell migration chamber with 8μm pores, the migration of uninfected wild-type and SHP-$2^{-/-}$ (Δ46-110) MEF cells was compared with the migration of the PZR isoform expressing MEF cell lines on BSA or fibronectin. As shown in Figure 9b, no significant migration was observed using BSA as the chemotactic stimulus. In contrast, in 3 independent experiments, migration was increased to variable levels with all cell lines using fibronectin as the integrin-

mediated stimulus. Importantly, a two to five-fold enhancement in migration was observed in the wild-type PZR-rescue MEF cell line compared to other PZR isoforms in SHP-2 rescue and mutant MEF cell lines. These results demonstrate that the intact PZR cytoplasmic domain containing the ITIM-motifs is important in modulating fibronectin-mediated cell migration rates, in these murine mesenchymal derived MEF cells.

DISCUSSION

PZR has previously been identified as a SHP-2 binding partner in epithelial cells [17]. In this paper, we report the identification and cloning of two novel isoforms of PZR, PZRa and PZRb, and demonstrate that these three isoforms are differentially expressed in the hematopoietic lineage and in stromal/mesenchymal cells. Of particular interest is the observation that the PZR isoforms are more strongly expressed on $CD34^{+}CD38^{+}$ clonogenic haematopoietic precursors than in more primitive $CD34^{+}CD38^{lo/-}$ pre-CFU precursors. Furthermore, PZR predominates over PZRb in endothelial cells. In addition, a switch occurs during monocytic differentiation when the ratio of PZR increases relative to PZRb. In mesenchymal cells and osteoblasts, PZR is the major isoform. The significance of the alteration in expression of the PZR isoforms during monocytic differentiation appears to be related to the structural differences between the different isoforms. While all three isoforms possess identical extracellular and transmembrane sequences, only the PZR isoform contains a cytoplasmic tail with two ITIM motifs ($VIY^{246}AQL$ and $VVY^{263}ADI$) that can specifically interact with SH2 domains of SHP-2 [17]. This in turn may endow PZR, but not PZRa or PZRb, with a negative SHP-2 regulatory role in these cells. It further implies that the differential expression of PZR isoforms may differentially modulate signaling pathways that involve SHP-2 in different cell types. During the preparation of this manuscript Zhao et al. [31] demonstrated that truncation of the intracellular domain of PZR blocks ConA induced PZR tyrosine phosphorylation in epithelial cells. A similar phenomenon may occur during myeloid differentiation from multipotent progenitors when a switch from PZR to PZRb occurs. We have demonstrated that PZR isoforms are generated by differential splicing of a single gene transcription unit on human chromosome 1q24. Other ITIM containing IgSF members (e.g. KIRS, ILTs.LIRs/MIRs, LAIR-1 and NKp46, CEACAMs and Siglecs) with both IgV and IgC2 domains are concentrated on human chromosome 19, while those with a single IgV domain (e.g. Myelin P0, PD-1, CMRF-35 and NKp44) like PZR are distributed across chromosomes 1, 2, 6 and 7 [32]. Interestingly, the PZR gene is closely linked to molecules (e.g myelin P0) on chromosome 1 with which it shares homology, suggesting that these molecules may have similar or related functions. It has been suggested recently that myelin P0 has a crucial role myelin production, with mutations in the myelin P0 extracellular, transmembrane or ITIM regions leading to inherited neuropathies (e.g. Dejerine-Sottas syndrome and Charcot-Marie-Tooth disease) [33, 34]. Similar mutations in PZR resulting in human disease have not been identified.

SHP-2 plays a critical role in haematopoietic and vascular development. Whether SHP-2 expresses its function in stem/progenitor cell or mesenchymal/osteoblast proliferation, survival, migration or differentiation is not fully established. The identification of its interacting partners and their mechanisms of action is therefore of major importance in determining its function and that of the PZR isoforms. Those partner molecules identified to date include certain cytokine receptors and

integrins [8, 9, 35]. SHP-2 physically interacts with and is tyrosine phosphorylated by the c-kit receptor tyrosine kinase upon of SCF ligand binding to hematopoietic and embryonic stem (ES) cells [36]. Treatment of ES cells with SCF induces Erk kinase activation, but this induction is completely blocked in *shp-2* $^{-/-}$ ES cells. SHP-2 also interacts with the common gp130 subunit of the IL-6, LIF and oncostatin M receptors [8, 12]. Thus, mutant ES cells lacking the SHP-2 binding site in either SHP-2 or gp130 have impaired abilities to differentiate *in vitro* [37]. It has also been shown that SHP-2 has an important role in cell motility. *Shp-2* mutant cells have defects in migration as well as spreading and have an increased number of focal adhesions [38]. Dominant negative SHP-2 expression blocks FGF- induced elongation of X*enopus* animal caps and prevents completion of gastrulation [2, 39]. A positive-feed back model is also suggested, in which integrin engagement induces c-Src to catalyze the tyrosyl phosphorylation of SHP-2 substrates, thereby recruiting SHP-2 to the plasma membrane. By further activating Src PTKs, SHP-2 transduces positive signals for downstream events such as MAPK activation and this alters cell shape [2].

Whether the ITIM-containing PZR, or PZRa and PZRb ITIM-less isoforms have a function in modulating these cytokine and adhesive responses has been a matter of speculation. We would predict that PZR, because of its distribution pattern, acts as a docking molecule for SHP-2 and prevents or rapidly down-modulates cytokine receptor and integrin interactions with SHP-2, following binding of their ligands. PZRa and PZRb, on the other hand, may act as activating molecules for ITAM containing partners. This would be reminiscent of the SIRP family of molecules, which consist of two subtypes distinguished by the presence (SIRPα) or absence (SIRPβ) of a cytoplasmic ITIM domain. Overexpression of SIRPα1 leads to the inhibition of cell activation induced by insulin, epidermal growth factor and platelet derived growth factor [40, 41]. It has also been shown that SIRPα1 can positively regulate the mitogen activated protein kinase (MAPK) signaling pathway in response to insulin and potentiate integrin-induced MAPK activation [42-44]. In contrast, SIRPβ1 physically associates with the killer cell activating receptor-associated protein (KARAP)/DAP-12 resulting in the functional coupling of SIRP1β to the protein tyrosine kinase Syk and to serotonin release and activation of the cells [45]. Alternatively, the PZRa and PZRb ITIM-less isoforms could directly interact with PZR and inhibit the ability of PZR to interact with SHP-2. In this paper, we have clearly demonstrated the importance of SHP-2 in regulating cell motility in our Boyden chamber transwell assays. In general, mutant SHP-2 (Δ46-110) displayed a decreased capacity to migrate in comparison to the rescue SHP-2 cell lines. Interestingly, the SHP-2 rescue cells expressing the full-length PZR isoform exhibited a five fold increase in their capacity to migrate on fibronectin. This is of particular interest since the full length PZR isoform contains tandem ITIMs that act as a docking site for SHP-2. Recent studies show that SHP-2 is involved in the deactivation of focal adhesion kinase (FAK) which is required for the generation of active FAK in the turnover of focal adhesions during migration [30]. SHP-2 also negatively regulates signaling

pathways that promote migration by reducing integrin-mediated adhesion. Thus, integrin engagement by fibronectin may lead to tyrosine phosphorylation of PZR, and recruitment and activation of SHP-2, which then induces dephosphorylation events to induce turnover of focal adhesions, reduced adhesion and increased cell motility. Our studies, therefore indicate that the cytoplasmic region of PZR containing ITIMs plays an important role in regulating integrin-mediated cell motility and that truncated forms of PZR lacking ITIMs fail to regulate cell motility. Recent studies [31] also indicate that PZR is a receptor for ConA on epithelial cells and that expression of a truncated form of PZR in an epithelial cell line is able to inhibit ConA-induced tyrosine phosphorylation of PZR. Our unique WM78 mAb has the ability to bind and tyrosine phosphorylate PZR (our unpublished data) and is undoubtedly more specific for PZR than ConA. Such a mAb will be useful for studying PZR specific activation both in haematopoietic and epithelial cells and may have therapeutic applications. A detailed analysis of the mechanisms of action of the PZR isoforms and of the WM78 mAb will therefore be the subject of further publications and experimentation.

ACKNOWLEDGMENTS

The authors wish to thank Dr Sharon Horseley for the chromosomal analysis, Guang-qian Zhou and Mrs Shira Gal for assistance with the DIG labeling and TaqMan analysis respectively, Mr Robin Roberts-Gant for help with the figures and Professors L.B To and M. Contreras for their continued support. This study was supported by grants from the Anti-Cancer Foundation of the Universities of South Australia, the NSW Cancer Council and the National Health and Medical Research Council of Australia (PJS, ACWZ and LJB) and by the National Blood Service, the Leukaemia Research Fund and Medical Research Council, UK (SMW and MR).

REFERENCES

1 Fauman, E. B. and Saper, M. A. (1996) Structure and function of the protein tyrosine phosphatases. Trends Biochem Sci **21**, 413-7

2 Oh, E. S., Gu, H., Saxton, T. M., Timms, J. F., Hausdorff, S., Frevert, E. U., Kahn, B. B., Pawson, T., Neel, B. G. and Thomas, S. M. (1999) Regulation of early events in integrin signaling by protein tyrosine phosphatase SHP-2. Mol Cell Biol **19**, 3205-15.

3 Tonks, N. K. and Neel, B. G. (1996) From form to function: Signalling by protein tyrosine phosphatases. Cell **87**, 365-68

4 Huyer, G. and Alexander, D. R. (1999) Immune signalling: SHP-2 docks at multiple ports. Curr Biol **9**, R129-32.

5 Klingmuller, U. (1997) The role of tyrosine phosphorylation in proliferation and maturation of erythroid progenitor cells--signals emanating from the erythropoietin receptor. Eur J Biochem **249**, 637-47.

6 Qu, C. K., Shi, Z. Q., Shen, R., Tsai, F. Y., Orkin, S. H. and Feng, G. S. (1997) A deletion mutation in the SH2-N domain of Shp-2 severely suppresses hematopoietic cell development. Mol Cell Biol **17**, 5499-507.

7 Kim, C. H., Qu, C. K., Hangoc, G., Cooper, S., Anzai, N., Feng, G. S. and Broxmeyer, H. E. (1999) Abnormal chemokine-induced responses of immature and mature hematopoietic cells from motheaten mice implicate the protein tyrosine phosphatase SHP-1 in chemokine responses. J Exp Med **190**, 681-90.

8 Frearson, J., A. and Alexander, D. R. (1997) The role of phosphotyrosine phosphatases in haematopoietic cell signal transduction. BioEssays **15**, 414-427

9 Yokoyama, W. M. (1997) What goes up must come down: the emerging spectrum of inhibitory receptors. J Exp Med **186**, 1803-8.

10 Frearson, J. A. and Alexander, D. R. (1998) The phosphotyrosine phosphatase SHP-2 participates in a multimeric signaling complex and regulates T cell receptor (TCR) coupling to the Ras/mitogen-activated protein kinase (MAPK) pathway in Jurkat T cells. J Exp Med **187**, 1417-26.

11 Feng, G. S. (1999) Shp-2 tyrosine phosphatase: signaling one cell or many. Exp Cell Res **253**, 47-54.

12 Plas, D. R. and Thomas, M. L. (1998) Negative regulation of antigen receptor signaling in lymphocytes. J Mol Med **76**, 589-95.

13 Saxton, T. M., Henkemeyer, M., Gasca, S., Shen, R., Rossi, D. J., Shalaby, F., Feng, G. S. and Pawson, T. (1997) Abnormal mesoderm patterning in mouse embryos mutant for the SH2 tyrosine phosphatase Shp-2. Embo J **16**, 2352-64.

14 Shi, Z. Q., Lu, W. and Feng, G. S. (1998) The Shp-2 tyrosine phosphatase has opposite effects in mediating the activation of extracellular signal-regulated and c-Jun NH2-terminal mitogen-activated protein kinases. J Biol Chem **273**, 4904-8

15 Raabe, T., Riesgo-Escovar, J., Liu, X., Bausenwein, B. S., Deak, P., Maroy, P. and Hafen, E. (1996) DOS, a novel pleckstrin homology domain-containing protein required for signal transduction between sevenless and Ras1 in Drosophila. Cell **85**, 911-20

16 Vivier, E. and Daeron, M. (1997) Immunoreceptor tyrosine-based inhibition motifs. Immunol Today **18**, 286-91

17 Zhao, Z. J. and Zhao, R. (1998) Purification and cloning of PZR, a binding protein and putative physiological substrate of tyrosine phosphatase SHP-2. J Biol Chem **273**, 29367-72.

18 Zhao, R. and Zhao, Z. J. (2000) Dissecting the interaction of SHP-2 with PZR, an immunoglobulin family protein containing immunoreceptor tyrosine-based inhibitory motifs. J Biol Chem **275**, 5453-9.

19 Chan, J. Y., Prudhoe, J. E., Jorgensen, B., Doyonnas, R., Zannettino, A. C. W., Buckle, V. J., Ward, C. J., Simmons, P. J. and Watt, S. M. (2001) Relationship between novel isoforms, functionally important domains, and subcellular distribution of novel CD164/endolyn. Blood **276**, 2139-2152

20 Watt, S. M., Bulter, L., Tavian, M., Burhing, H.-J., Rapppold, I., Simmons, P. J., Zannettino, A. C. W., Buck, D., Fuchs, A., Doyonnas, R., Chan, J. Y.-H., Levesque, J.-P., Peault, B. and Roxanis, I. (2000) Functionally defined CD164 epitopes are expressed on CD34+ cells throughoutonogeny but display distinct distribution patterns in adult hematopoietic and nonhematopoietic tissues. Blood **95**, 3113-3124

21 Watt, S. M., Buhring, H. J., Rappold, I., Chan, J. Y., Lee-Prudhoe, J., Jones, T., Zannettino, A. C., Simmons, P. J., Diyonnas, R., Sheer, D. and Bulter, L. H. (1998) CD164, a novel sialomucin on CD34(+) and erythroid subsets, is located on human chromosome 6q21. Blood **92**, 849-66

22 Ford, A. M., Watt, S. M., Furley, A. J., Molgaard, H. V. and Greaves, M. F. (1988) Cell lineage specificity of chromatin configuration around the immunoglobulin heavy chain enhancer. Embo J **7**, 2393-9

23 Zannettino, A. C. W., Buhring, H.-J., Niutta, S., Watt, S. M., Benton, M. A. and Simmons, P. J. (1998) The sialomucin CD164 (MGC-24v) is an adhesive glycoprotein expressed by human hematopoietic progenitors and bone marrow stromal cells that serves as potential negative regulator of hematopoiesis. Blood **92**, 2613-2628

24 Simmons, P. J., Przepiorka, D., Thomas, E. D. and Torok-Storb, B. (1987) Host origin of marrow stromal cells following allogeneic bone marrow transplantation. Nature **328**, 429-32.

25 Haylock, D. N., To, L. B., Dowse, T. L., Jutter, C. A. and Simmons, P. J. (1992) Ex-vivo expansion and maturation of peripheral blood CD34+ cells into myeloid lineage. Blood **80**, 1405-12

26 Cole, S. R., Ashman, L. K. and Ey, P. L. (1987) Biotinylation: an alternative to radioiodination for the identification of cell surface antigens in immunoprecipitates. Mol Immunol **24**, 699-705.

27 Laemmli, U. K. (1970) Cleavage of structural proteins during the assembly of the head of bacteriophage T4. Nature **227**, 680-5.

28 Zannettino, A. C. W., Rayner, J. R., Ashman, L. K. G., T.J. and Simmons, P. J. (1996) A powerfull new technique for isolating genes encoding cell surface antigen using retroviral expression cloning. Journal of Immunology **156**, 611

29 Chiu, R. W., Murphy, M. F., Fidler, C., Wainscoat, J. S. and Lo, Y. M. (2001) Technical optimization of RhD zygosity determination by real-time quantitative polymerase chain reaction: implication for fetal RhD status determination by maternal plasma. Ann N Y Acad Sci **945**, 156-60

30 Yu, D. H., Qu, C. K., Henegariu, O., Lu, X. and Feng, G. S. (1998) Protein-tyrosine phosphatase Shp-2 regulates cell spreading, migration, and focal adhesion. J Biol Chem **273**, 21125-31

31 Zhao, R., Guerrah, A., Tang, H. and Zhao, Z. J. (2001) Cell surface glycoprotein PZR is a major mediator of concanavalin A-induced cell signaling. J Biol Chem **20**, 20

32 Fournier, N., Chalus, L., Durand, I., Garcia, E., Pin, J. J., Churakova, T., Patel, S., Zlot, C., Gorman, D., Zurawski, S., Abrams, J., Bates, E. E. and Garrone, P. (2000) FDF03, a novel inhibitory receptor of the immunoglobulin superfamily, is expressed by human dendritic and myeloid cells. J Immunol **165**, 1197-209.

33 Xu, M., Zhao, R., Sui, X., Xu, F. and Zhao, Z. J. (2000) Tyrosine phosphorylation of myelin P(0) and its implication in signal transduction. Biochem Biophys Res Commun **267**, 820-5.

34 Xu, W., Shy, M., Kamholz, J., Elferink, L., Xu, G., Lilien, J. and Balsamo, J. (2001) Mutations in the cytoplasmic domain of P0 reveal a role for PKC- mediated phosphorylation in adhesion and myelination. J Cell Biol **155**, 439-46.

35 Mizuno, K., Tagawa, Y., Mitomo, K., Arimura, Y., Hatano, N., Katagiri, T., Ogimoto, M. and Yakura, H. (2000) Src homology region 2 (SH2) domain-containing phosphatase-1 dephosphorylates B cell linker protein/SH2 domain leukocyte protein of 65 kDa and selectively regulates c-Jun NH2-terminal kinase activation in B cells. J Immunol **165**, 1344-51.

36 Qu, C. K., Yu, W. M., Azzarelli, B., Cooper, S., Broxmeyer, H. E. and Feng, G. S. (1998) Biased suppression of hematopoiesis and multiple developmental defects in chimeric mice containing Shp-2 mutant cells. Mol Cell Biol **18**, 6075-82.

37 Burdon, T., Stracey, C., Chambers, I., Nichols, J. and Smith, A. (1999) Suppression of SHP-2 and ERK signalling promotes self-renewal of mouse embryonic stem cells. Dev Biol **210**, 30-43.

38 Yu, C., Jin, Y. Burakoff, S. (2000) Cytosolic Tyrosine dephosphorylation of STAT5 Potentila role of SHP-2 in STAT-5 regulation. Journal of Biological Chemistry **275**, 599-604

39 Tang, T. L., Freeman, R. M., Jr., O'Reilly, A. M., Neel, B. G. and Sokol, S. Y. (1995) The SH2-containing protein-tyrosine phosphatase SH-PTP2 is required upstream of MAP kinase for early Xenopus development. Cell **80**, 473-83.

40 Kharitonenkov, A., Chen, Z., Sures, I., Wang, H., Schilling, J. and Ullrich, A. (1997) A family of proteins that inhibit signalling through tyrosine kinase receptors. Nature **386**, 181-6.

41 Fujioka, Y., Matozaki, T., Noguchi, T., Iwamatsu, A., Yamao, T., Takahashi, N., Tsuda, M., Takada, T. and Kasuga, M. (1996) A novel membrane glycoprotein, SHPS-1, that binds the SH2-domain- containing protein tyrosine phosphatase SHP-2 in response to mitogens and cell adhesion. Mol Cell Biol **16**, 6887-99.

42 Seiffert, M., Brossart, P., Cant, C., Cella, M., Colonna, M., Brugger, W., Kanz, L., Ullrich, A. and Buhring, H. J. (2001) Signal-regulatory protein alpha (SIRPalpha) but not SIRPbeta is involved in T-cell activation, binds to CD47 with high affinity, and is expressed on immature CD34(+)CD38(-) hematopoietic cells. Blood **97**, 2741-9.

43 Tomasello, E., Cant, C., Buhring, H. J., Vely, F., Andre, P., Seiffert, M., Ullrich, A. and Vivier, E. (2000) Association of signal-regulatory proteins beta with KARAP/DAP-12. Eur J Immunol **30**, 2147-2156

44 Takada, T., Matozaki, T., Takeda, H., Fukunaga, K., Noguchi, T., Fujioka, Y., Okazaki, I., Tsuda, M., Yamao, T., Ochi, F. and Kasuga, M. (1998) Roles of the complex formation of SHPS-1 with SHP-2 in insulin- stimulated mitogen-activated protein kinase activation. J Biol Chem **273**, 9234-42.

45 Tomasello, E., Olcese, L., Vely, F., Geourgeon, C., Blery, M., Moqrich, A., Gautheret, D., Djabali, M., Mattei, M. G. and Vivier, E. (1998) Gene structure, expression pattern, and biological activity of mouse killer cell activating receptor-associated protein (KARAP)/DAP-12. J Biol Chem **273**, 34115-9.

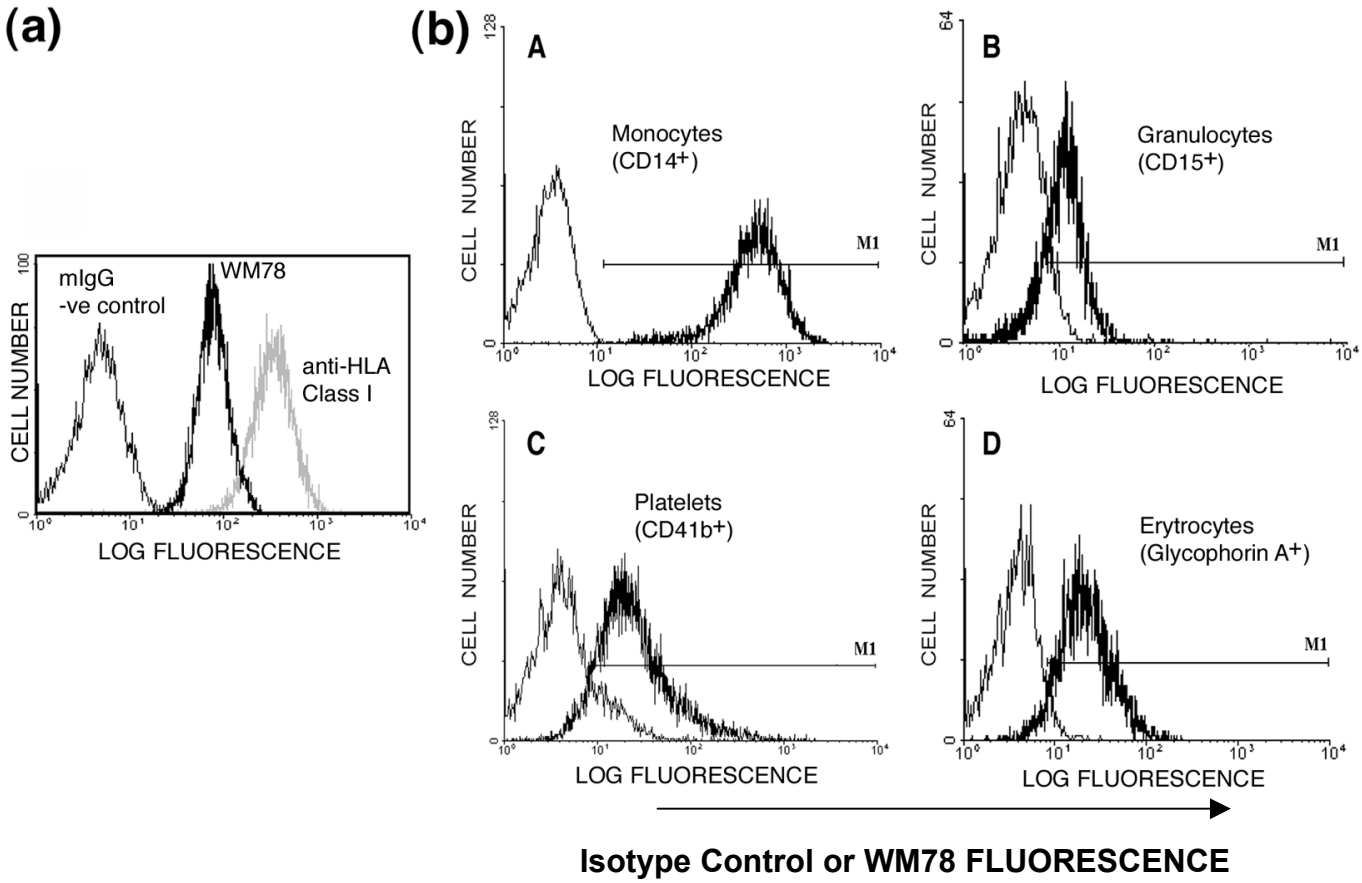

(c)

Percentage WM78 Positive Cells in each Subset after gating against a Negative Isotype Control	
Cellular subset	**Percentage Positive Mean ± SEM (n=3)**
$CD14^+$ monocytes	99.3±1.2
$CD15^+$ granulocytes	42.5±12.6
$CD19^+$ B cells	75.6±18.4
Glycophorin A+ erythrocytes	73.2±23.2
$CD4^+$ T cells	41.1±10.3
$CD8^+$ T cells	38.2±6.2
$CD41b^+$ platelets	57.9±13.2
$CD56^+$ natural killer cells	49.9±15.3

Figure 1: The WM78 mAb identifies an antigen on cultured human bone marrow SOB and peripheral blood cells

Single color flow cytometry showing binding of the mAb WM78 (bold histograms) to cultured human bone marrow SOB cells (a). Representative histograms of peripheral blood myeloid subsets gated for CD14, CD15, CD41b or anti-glycophorin positive cells prior to analysis with the isotype matched negative control (non-bold histograms) or the WM78 mAb (bold histograms) (b). The non-binding, isotype matched mIgG1 negative control mAb was 1B5 (non-bold histograms). The anti-HLA Class I mAb was used as the positive control (a). M1 marks the position of the positive gate used to determine the % positive cells in each subset. (c) The table shows the percent of each peripheral blood cell subset that stains with WM78 after gating against a negative isotype control. Values are mean ± SEM for 3 independent experiments.

(a)

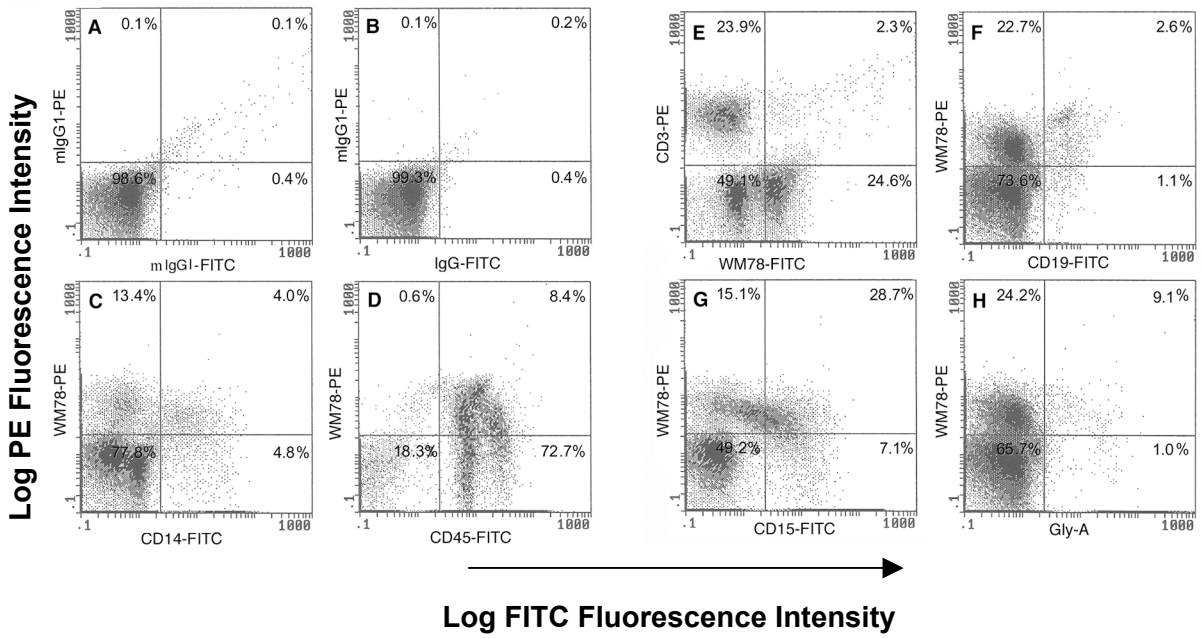

(b)

Percentage WM78 Positive Cells in each Subset after gating against a Negative Isotype Control	
Cellular subset	**Percentage Positive Mean ± SEM (n=3)**
$CD14^+$ monocytes	54.9±18.5
$CD15^+$ granulocytes	23.3±3.2
$CD19^+$ B cells	69.6±3.3
Glycophorin A+ erythrocytes	12.7±4.0
$CD3^+$ T cells	14.9±5.9
$CD45^+$ leukocytes	14.1±5.5

Figure 2: Differential binding of the WM78 mAb to human bone marrow hematopoietic cell subsets. Representative two-colour dot plots demonstrating the differential binding of CD markers and the WM78 mAb to BMMNC (a). The cells were labeled with FITC conjugated lineage specific markers and biotin conjugated WM78 mAb plus PE-streptavidin. Mouse IgG1 mAbs conjugated with PE, FITC or biotin were used as negative controls. The % in each quadrant represents the percentage of BMMNC staining with the mAbs indicated. (b) cells were gated for each of the positive CD markers separately and the relative percentage of $CD14^+$, $CD45^+$, $CD3^+$, $CD19^+$, $CD15^+$ and glycophorin A^+ cells staining with WM78 determined. Values are mean ± SEM for 3 independent experiments.

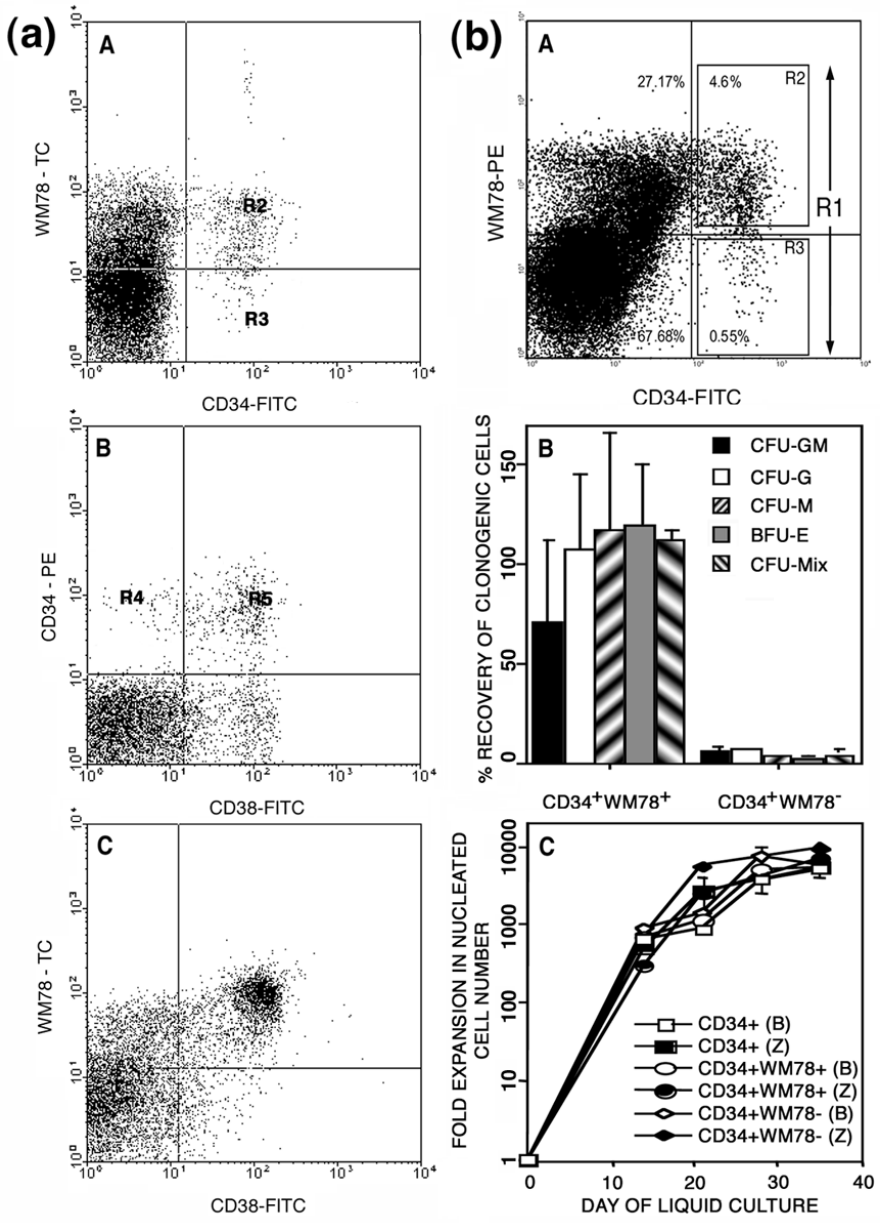

Figure 3: The WM78 mAb binds differentially to $CD34^+CD38^+$ and $CD34^+CD38^{lo/-}$ subsets and to hematopoietic progenitor cells. (a) A typical two-colour dot plot of BMMNC labeled with WM78-biotin plus streptavidin-Tricolour, CD34-FITC and CD38-PE (A), CD34-PE, CD38-FITC and WM78-biotin plus streptavidin-Tricolour (B) and WM78-biotin plus streptavidin-Tricolour, CD38-FITC and CD34-PE (C). The relative CD38 staining of cells in the $CD34^+WM78^+$ and $CD34^+WM78^{lo/-}$ (A) and the relative WM78 staining of cells in $CD34^+CD38^+$ and $CD34^+CD38^{lo/-}$ fractions (B) were determined by flow cytometry as median fluorescence values (MFI) for 3 independent samples. (b) A: A representative dot plot of BMMNC labeled with WM78-biotin plus streptavidin-PE and CD34-FITC and flow sorted into the $CD34^+$ (Region R1), $CD34^+WM78^+$ (Region R2) and $CD34^+WM78^-$ (Region R3) subsets, showing the percentages in each quadrant. B: Clonogenic cells were measured from sorted fractions, R1, R2 and R3, and analyzed for the presence of day 14 multipotential, erythroid and myeloid progenitor cell [Solid (CFU-GM), open (CFU-G), left hatched (CFU-M), stippled (BFU-E) and right hatched (CFU-Mix)]. Results (means ± S.E.M. from 3 donors R, B and Z) are expressed as the recovered clonogenic cells in fractions R2 and R3 on the basis of the percentage of $WM78^+$ or $^{lo/-}$ cells in the $CD34^+$ fraction R1 and after normalization of values for clonogenic cell output to the $CD34^+$ subset to 100%. C: Cells from 2 donors B and Z sorted into fractions R1, R2 and R3 were also assayed for their content of pre-CFU as described in the Materials and Methods. Data represent the fold expansion of nucleated cells after 1000 cells from each fraction was cultured in 6HGF for up to 35 days.

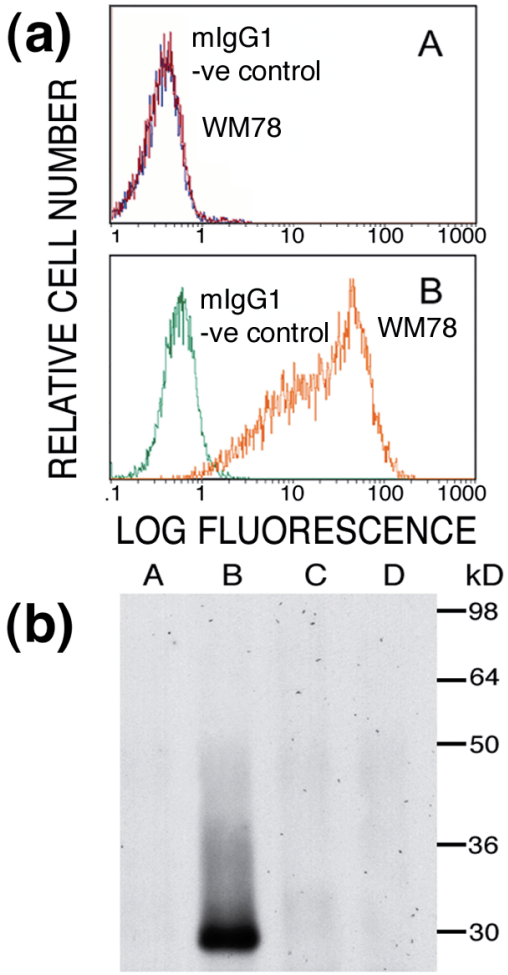

Figure 4: Identification of PZRb. (a) After expression cloning, PZRa cDNA was transfected into FDCP-1 cells and analyzed by flow cytometry for cell surface binding of the WM78 mAb or a mIgG1 isotype matched negative control (B). The histograms in (A) represents sham transfected FDCP-1 cells labeled with mIgG1 or WM78 mAbs. (b) Immunoprecipitation of the PZRa molecule using mIgG1 (lanes A and C) or the WM78 mAb (lanes B and D) from FDCP-1 cells expressing PZRa (lanes A and B) or in non–expressing FDCP-1 cells (lanes C and D) and analysis by 10% SDS-PAGE.

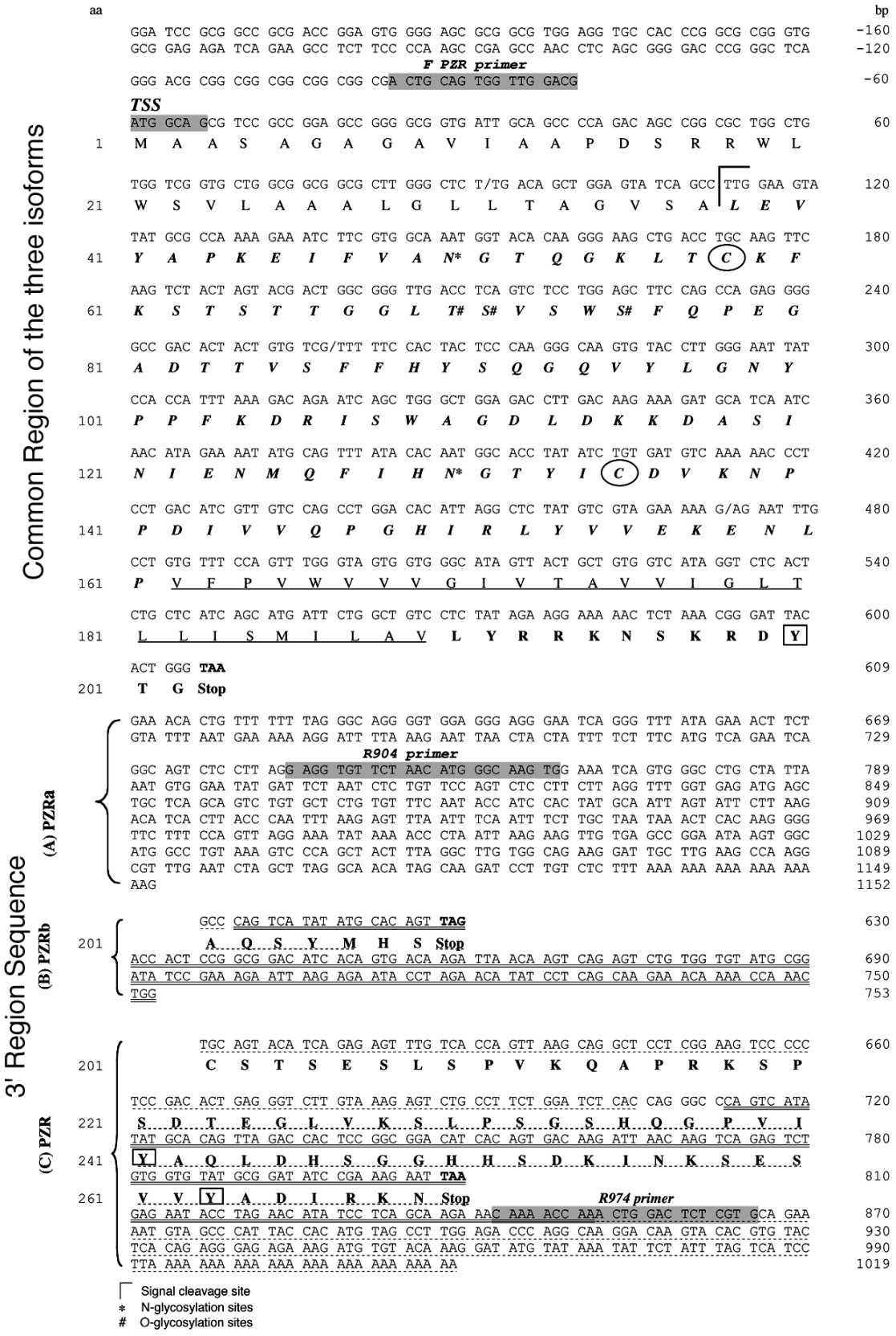

Figure 5: Comparative cDNA and amino acid sequences of PZR isoforms. The PZR cDNA sequence was obtained by RT-PCR analyses using primers indicated. The extracellular, the transmembrane and the intracellular domains are indicated by bold italics, underlined, and bold respectively. Cysteines are circled and tyrosine residues are marked in a square. Potential N- and O- linked glycosylation sites are indicated by * and # respectively. Differences between the cytoplasmic domains of PZR, PZRa and PZRb isoforms are dot underlined and identities in the 3' region between PZR and RZRb are double underlined. The positions of FPZR, R904 and R974 primers are highlighted. The additional 5' UTR and 3' UTR sequences of PZRa were identified from the PZRa cDNA sequence. The 3' UTR sequence of PZR was obtained from the published sequence (Gene Bank Accession number: AF087020).

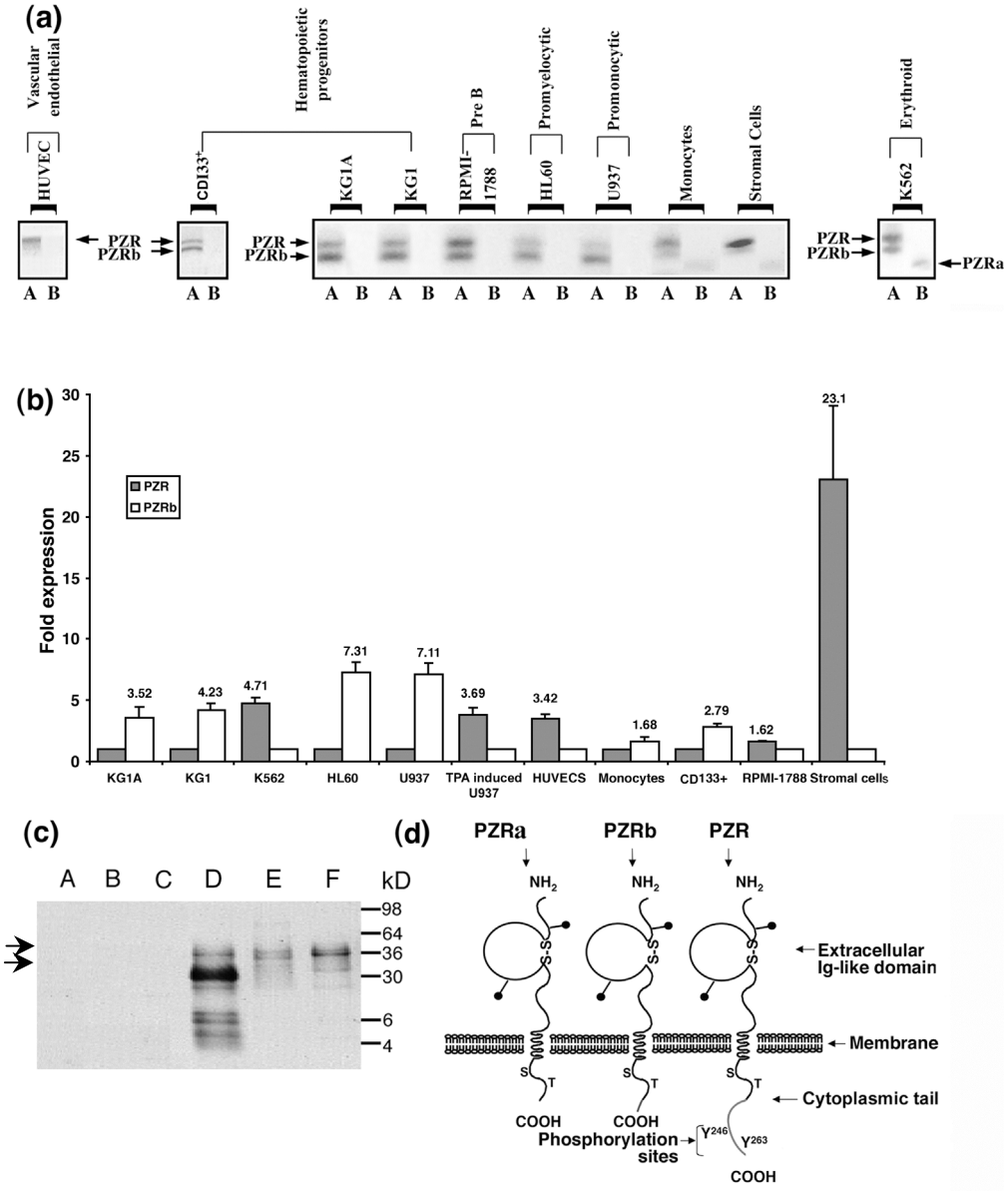

(e)

PZR amino acid identities and similarities with:	***PZR***							
	Whole peptide		*Extracellular domain*		*Transmembrane domain*		*Cytoplasmic domain*	
	Identity	*Similarity*	*Identity*	*Similarity*	*Identity*	*Similarity*	*Identity*	*Similarity*
PZRa	74.1%	74.8%	100.0%	100.0%	100.0%	100.0%	18.8%	18.8%
PZRb	74.8%	79.5%	100.0%	100.0%	100.0%	100.0%	18.8%	21.7%
Myelin P0	36.8%	53.5%	44.7%	61.7%	32.0%	53.4%	27.0%	42.0%
Epithelial V- like antigen	27.5%	40.5%	40.6%	55.2%	17.8%	42.8%	16.3%	22.5%

Figure 6: Distribution of hematopoietic endothelial and mesenchymal derived cells for PZR isoforms. (a) The distribution of PZR isoforms was examined by RT-PCR analysis in KG1A, KG1, HL60, U937, K562, RPMI-1788 as well as HUVEC, normal CD133$^+$ progenitor cells (95% purity), CD14$^+$ peripheral blood monocytes (86% purity) and cultured bone marrow SOB. (b) Real-Time Quantitative PCR. Fold expression of PZR versus PZRb is presented. Values are means of 4 independent experiments ±S.D. as calculated in Materials and Methods. (c) Immunoprecipitation of PZR isoforms from human bone marrow cultured stromal / osteoblast cells (lane D), CD34$^+$ cells (lane E) and the erythroid precursor cell line K562 (lane F) with the WM78 mAb and the respective negative controls (lanes A, B and C) and electrophoresis on 10% SDS-PAGE. Arrows indicate the positions of the predicted PZR and PZRb isoforms. Seablue II markers (Navex, Invitrogen, CA, USA) were used. (d) shows a schematic representation of PZR isoforms. (e) The percent amino acid identities and similarities between PZR and PZRa, PZRb, myelin P0 and epithelial V-like antigen are listed.

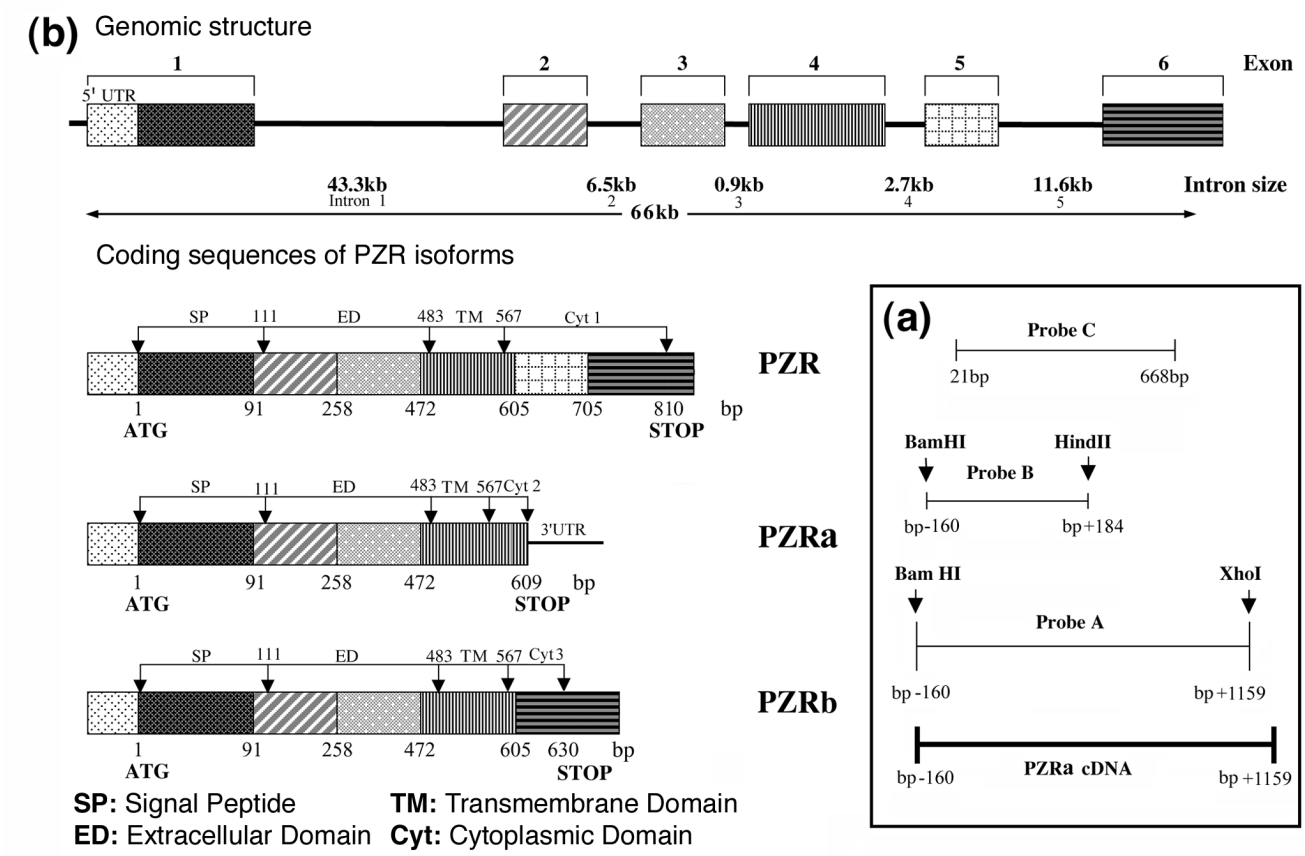

Figure 7: PZR genomic structure. (a) PZRa probes used for screening PAC and cosmid libraries. (b) schematic representation of the genomic structure of PZR gene showing exons 1 to 6 (boxed) and introns 1 to 5 (line). Sequences encoding the different domains (signal peptide (SP), extracellular (ED), transmembrane (TD) and cytoplasmic (cyt1, cyt2, cyt3) domains for PZR, PZRa and PZRb mRNAs are shown.

Biochemical Journal Immediate Publication. Published on 1 Nov 2002 as manuscript BJ20020935

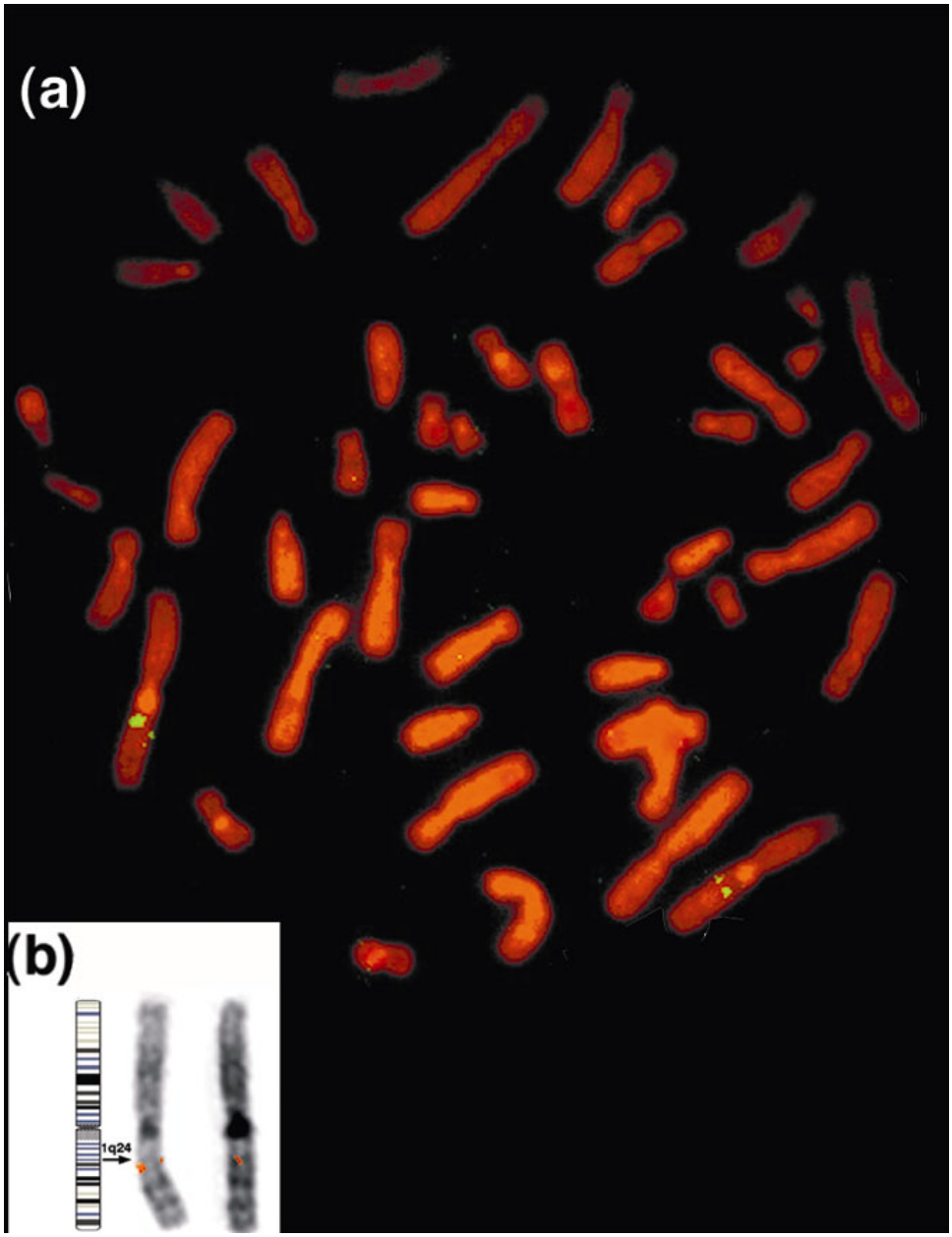

Figure 8: The PZR gene is located on human chromosome 1q24. (a) FISH analysis using the ah95b1 cosmid clone as a probe shows that PZRa, PZRb and PZR isoforms are located on human chromosome 1q24. (b) An ideogram of human chromosome 1 showing the localization of the PZR gene to band q24.

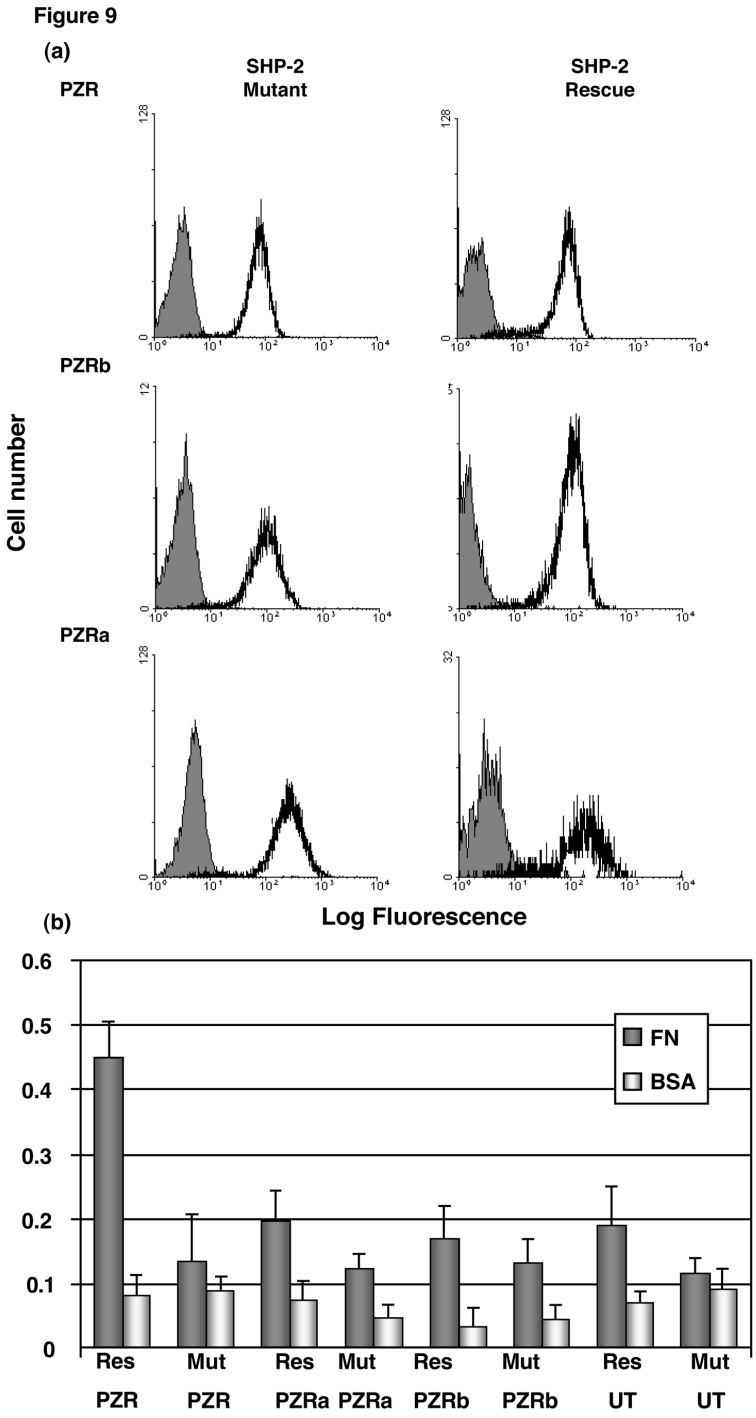

Figure 9: Cell motility regulated by PZR isoforms. (a) Surface expression of PZR isoform-expressing SHP-2 rescue ("wild type") and SHP-2 mutant (Δ46-110) MEF cell lines used in the assays. Cells were stained with 10 μg/ml of the PZR-specific mAb WM78 (white profile) or isotype control 1B5 (grey profile). Specific staining was detected after incubation with saturating levels of FITC-conjugated sheep anti-mouse Ig. These profiles show a comparable level of PZR expression for each of the different isoforms. (b) The effect of PZR isoforms on migration of SHP-2 rescue "wild type" (Res) and SHP-2 mutant (Δ46-110) (Mut) cell lines was assessed by the Boyden transwell assay. The cells stably transduced with various isoforms of PZR specified or non - transfected cells (UT) were seeded on 8 μm porous membranes coated with either BSA or fibronectin (FN) in Boyden multiwell chambers. Following incubation for 5 hrs at 37°C, cells which had migrated through the membrane were quantitated by crystal violet staining and spectrophotometry 600nm. A significant difference ($p<0.005$, Anova) in the migration potential was conferred to cells expressing the ITIM-containing isoform of PZR. The results represent the mean ± SEM of 3 independent experiments.